Agile UAV Landing on a Moving Maritime Vessel via MPC-Based Trajectory Generation

Ondřej Procházka, Filip Novák, Tomáš Báča, Parakh M. Gupta, Robert Pěnička, Martin Saska

***Abstract*—Autonomous landing of an Unmanned Aerial Vehicle (UAV) on a maritime vessel in harsh sea conditions is a critical capability for enabling persistent UAV operations at sea. We present a Model Predictive Controller (MPC)-based trajectory generation method that enables a multirotor UAV to land precisely and rapidly on the deck of a moving Autonomous Surface Vessel (USV), even when the deck is continuously tilting due to waves. The key novelty is a dynamic penalization scheme, which we named Forcing Attitude Alignment (FAA), that exponentially increases the weight on attitude-tracking as the UAV approaches the deck, driving attitude synchronization between the UAV and the USV upon touchdown. The MPC exploits full-state predictions of the USV, including position, orientation, and their first derivatives, and a three-phase state machine governs distinct flight behaviours from navigation through landing. Simulations across sea states up to Rough sea (wave height $4\,\mathrm{m}$) demonstrate a $100\,\%$ success rate in most scenarios, twice the touchdown precision, and $50\,\%$ faster landing than the studied state-of-the-art methods. Real-world experiments on a moving USV corroborate these results with all computation performed onboard the UAV in real time.**

***Index Terms*—unmanned aerial vehicle, unmanned surface vehicle, model predictive control, autonomous landing, maritime robotics, multi-robot systems**

Supplementary Material

Webpage: https://mrs.fel.cvut.cz/papers/mpc-traj-gen-for-landing

I. Introduction

Offshore infrastructure inspection, covering wind farms and oil platforms, increasingly relies on Unmanned Aerial Vehicles (UAVs) for tasks that are hazardous or inefficient for human operators [1]. Persistent UAV deployments require a carrier Autonomous Surface Vessel (USV) for transport, recharging [2], and payload exchange. The ability for a UAV to land autonomously on such a vessel in open-water conditions is therefore a fundamental capability for any practical offshore inspection system.

The following challenge arises. It is estimated that the probability of encountering waves exceeding $0.5\,\mathrm{m}$ in height is approximately $90\,\%$ worldwide [4]. Waves affect the USV's position, altitude, attitude, and velocity simultaneously. The USV slides (surge/sway), tilts (roll/pitch), and heaves, which makes the landing procedures challenging, especially on small USVs. Landing on such a platform demands both precise position tracking and attitude synchronization at touchdown to prevent the UAV from overturning and potentially falling overboard.

This work has been supported by the Technology Innovation Institute - Sole Proprietorship LLC, UAE, under the Research Project Contract No. TII/ARRC/2055/2021, CTU grant no SGS23/177/OHK3/3T/13 and the Czech Science Foundation (GAČR) under research project No. 23-06162M.

Fig. 1: Illustration of the landing task: (a) manual UAV landing in the real world [3], (b) autonomous landing in simulation under high waves, and (c) the UAV and USV platforms in the real world.

The communication link in cooperative UAV–USV inspection teams provides an opportunity most prior work does not exploit: sharing real-time full USV state beyond simple position. Most existing methods either wait for calm windows [5], rely on vision-only sensing that fails when the USV leaves the camera Field of View (FOV) [6], or use simplified vessel models ignoring surge, sway, and heave [7].

This workshop paper presents MPC-FAA, an Model Predictive Controller (MPC)-based trajectory generation method enabling agile, attitude-synchronized UAV landings on a moving USV without waiting for calm sea, by (i) using full USV states via a 6-degree of freedom (DOF) wave-augmented Fossen model [8], [9]; (ii) dynamically adjusting MPC penalization matrices per flight phase; and (iii) applying novel Forcing Attitude Alignment (FAA) method to synchronize UAV attitude with the deck before touchdown. Validated in over $1\,000$ simulations and real-world experiments, MPC-FAA achieves $2\times$ better touchdown accuracy and $50\,\%$ faster landing versus [5], with all computation onboard in real time. Full details appear in [10], this workshop paper highlights the core method and results most relevant to the aerial–maritime inspection community.

II. Related Work

Visual servoing approaches, both Position-Based visual servoing (PBVS) and Image-Based Visual Servoin (IBVS), can be used to land the UAV on tilting decks, but require continuous visual contact and assume small attitude deviations [11]–[14].

To enable landing without visual contact, Light Detection and Ranging (LiDAR)-based methods [7], [15] detect vessel motion and use Signal Prediction Algorithm (SPA) or Landing Period Indicator (LPI) algorithms to determine safe landing windows, including heave compensation. However, if the vessel leaves the sensor FOV, its global position becomes unknown. Wireless communication between UAV and USV for sharing global position is explored in [16], though Global Navigation Satellite System (GNSS) precision is insufficient for small UAVs.

MPC-based methods [5], [17] use predictive landing cost functions but condition descent on reduced deck tilt, which might result in long waiting times that are incompatible with time-limited inspection missions.

Our work differs from state-of-the-art methods in three ways: (a) *trajectory generation with dynamic penalization matrix adaptation* per flight phase, unique to our method; (b) *full attitude synchronization* at touchdown; and (c) uses a *6-DOF wave model* for USV prediction. Together, these enable landing without waiting for calm, reducing landing time by $50\,\%$ and doubling precision compared to [5].

III. Problem Formulation

A. USV and UAV Models

The 6 DOF model of the USV utilized in this work is composed of the standard Fossen's USV model [9] and the model of the waves as is proposed in [8]. According to [8], the general definition of the USV model is defined as

$$\dot{\boldsymbol{\eta}}_L = \boldsymbol{\nu}, \tag{1}$$

$$\dot{\boldsymbol{\nu}} = -\mathbf{M}^{-1}(\mathbf{D}\boldsymbol{\nu} + \mathbf{G}\boldsymbol{\eta}_L) + \mathbf{C}_{\text{wave},\boldsymbol{\nu}}\mathbf{x}_{\text{wave},\nu}, \tag{2}$$

$$\dot{\mathbf{x}}_{\text{wave},\nu} = \mathbf{A}_{\text{wave},\boldsymbol{\nu}}\mathbf{x}_{\text{wave},\nu}, \tag{3}$$

where $\boldsymbol{\eta}_L \in \mathbb{R}^3 \times \mathcal{S}^3$ contains positions and Euler angles, $\boldsymbol{\nu} \in \mathbb{R}^6$ contains linear and angular velocities, $\mathbf{M}$ is the total inertia, $\mathbf{D}$ is damping, $\mathbf{G}$ contains restoring forces. $\mathbf{A}_{\text{wave},\boldsymbol{\nu}}$ is the state-space matrix encoding the damping and frequency of the modeled waves, $\mathbf{C}_{\text{wave},\boldsymbol{\nu}}$ is the diagonal output matrix whose size corresponds to the number of modeled wave components, and $\mathbf{x}_{\text{wave},\nu}$ is the state vector comprising all individual wave component states. This model is used solely for onboard USV state estimation and prediction, without requiring actuator inputs, preserving robustness against communication degradation.

The UAV is modeled as a rigid-body quadrotor with translational and angular dynamics

$$\dot{\boldsymbol{\eta}}_{p_c} = \boldsymbol{\upsilon}_l, \qquad \ddot{\boldsymbol{\eta}}_{p_c} = -g\,\hat{\mathbf{e}}_3 + \mathbf{R}_c^w \tfrac{\mathbf{T_C}}{m}, \tag{4}$$

$$\dot{\boldsymbol{\eta}}_{o_c} = \boldsymbol{\upsilon}_a, \qquad \ddot{\boldsymbol{\eta}}_{o_c} = (\mathbf{T}_c^w \mathbf{I}_c \mathbf{T}_w^c)^{-1}(\boldsymbol{\tau_C} - \mathbf{C_t}\,\dot{\boldsymbol{\eta}}_{o_c}), \tag{5}$$

where $\boldsymbol{\eta}_{p_c}$, $\boldsymbol{\upsilon}_l$, $\boldsymbol{\eta}_{o_c}$, $\boldsymbol{\upsilon}_a$ are position, linear velocity, orientation (Euler angles), and Euler rates in world frame $\mathcal{W}$, g is gravitational acceleration, m mass, $\mathbf{R}_c^w$ the *xyz* Euler rotation, $\mathbf{T_C} = [0,\, 0,\, k_T \sum \omega_i^2]^\top$ the body-fixed thrust, $\boldsymbol{\tau_C}$ the rotor torque, $\mathbf{I}_c$ the inertia matrix, and $\mathbf{C_t}$ centripetal/gyroscopic terms [18]. Then the model is linearized such that it can be used within linear MPC, where full description can be found in [10].

B. MPC Trajectory Generation

We use a linear MPC in incremental input form to eliminate steady-state bias at hover. The augmented model includes the previous input as a state, the optimizer acts on increments $\Delta\mathbf{u}_{[t]} = \mathbf{u}_{[t]} - \mathbf{u}_{[t-1]}$. The objective minimizes tracking error against predicted USV states

$$\min_{\Delta\mathbf{u}} \; J = \tfrac{1}{2}\Delta\mathbf{u}^\top\big(\bar{\mathbf{C}}_a^\top \bar{\mathbf{Q}}_{[t]} \bar{\mathbf{C}}_a + \bar{\mathbf{R}}\big)\Delta\mathbf{u} + \mathbf{f}^\top\Delta\mathbf{u}, \tag{6}$$

where $\bar{\mathbf{C}}_a$ denotes the controllability matrix of the augmented model of the UAV and

$$\mathbf{f}^\top = \begin{bmatrix}\mathbf{x}_{[t]}^\top & \mathbf{u}_{[t-1]}^\top & \mathbf{r}_{[t]}^\top\end{bmatrix}\begin{bmatrix}\bar{\mathbf{A}}_a^\top \bar{\mathbf{Q}}_{[t]} \bar{\mathbf{C}}_a \\ -\bar{\mathbf{T}}\bar{\mathbf{C}}_a\end{bmatrix}^\top \tag{7}$$

is the linear cost term encoding the current UAV state $\mathbf{x}_{[t]}$, previous input $\mathbf{u}_{[t-1]}$, and the USV reference trajectory $\mathbf{r}_{[t]}$. $\bar{\mathbf{A}}_a$ is the column-stacked propagation matrix of the augmented model over the horizon and matrices $\bar{\mathbf{Q}}$, $\bar{\mathbf{T}}$ and $\bar{\mathbf{R}}$ were obtained from a simplified simultaneous form of the standard objective function [19]. Subject to state and slew-rate constraints, the predicted trajectory is composed of $N = 20$ steps at $50\,\text{ms}$ each ($2\,\text{s}$ total). The critical feature is that $\mathbf{Q}_{[t]}$ is *time-varying* and adapted per flight phase.

C. Forcing Attitude Alignment (FAA)

During the Flare phase, the penalization weights on roll and pitch errors in $\mathbf{Q}_{[t]}$ grow exponentially as the UAV closes on the deck

$$f(v_d) = 1 + \frac{\alpha}{e^{\beta v_d}}, \tag{8}$$

where v_d is the remaining vertical distance to the deck, and α, β are empirically tuned. As $v_d \to 0$, attitude weights dominate, driving roll and pitch to match the USV's deck tilt before contact. This can only be applied because the vertical approach speed is independently regulated to a constant value. As a result, we get a smooth touchdown trajectory on a tilted deck with negligible position penalty.

D. State Machine and Flight Phases

We consider the UAV landing procedure to have three phases: NAVIGATION, FOLLOW, and LANDING. Individual phases are further divided into states, which are explained in the following paragraphs and shown in Figure 2.

NAVIGATION: The UAV climbs to approach altitude $h_a = 15\,\text{m}$ and flies toward the USV using GNSS position, keeping the USV in the camera FOV.

FOLLOW: On visual contact (AprilTag or UltraViolet Direction And Ranging (UVDAR) [20]), the UAV follows at $h_t = 7\,\text{m}$, matching USV horizontal velocity. The landing phase is entered based on the distance, trajectory feasibility, and predefined covariance limits.

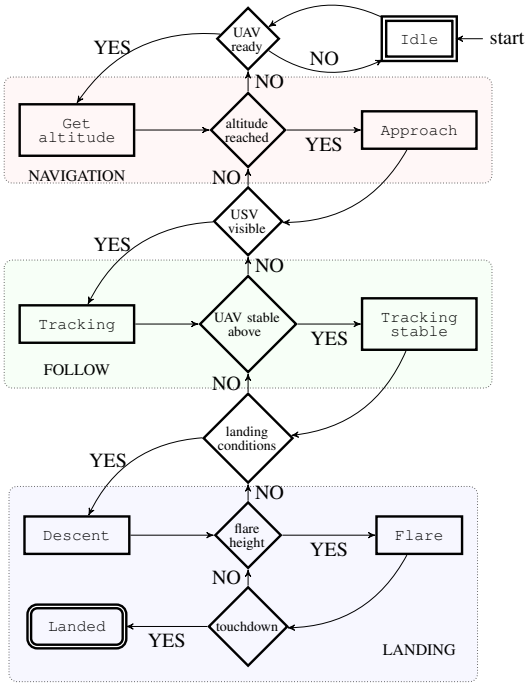

Fig. 2: Illustration of the developed state machine composed of three phases ensures decision-making throughout the whole process. Adopted from [10].

LANDING: Descent at $v_{la} = 1\,\mathrm{m\,s^{-1}}$, at flare height the MPC reference switches to full predicted USV pose and FAA activates. Touchdown is confirmed via accelerometers and a rangefinder. Loss of USV aborts to Follow.

IV. Experiments and Results

A. Simulation Setup

Experiments were conducted in a Gazebo-based simulator using Gerstner wave modeling [21] integrated with the Multi-robot Systems (MRS) UAV system [22]. Three wave components simulate realistic offshore conditions. The UAV weighs $3.5\,\mathrm{kg}$ with $0.325\,\mathrm{m}$ arm length; the USV is $5\,\mathrm{m}\times2.5\,\mathrm{m}$, $180\,\mathrm{kg}$, with a $2.5\,\mathrm{m}\times1.7\,\mathrm{m}$ landing deck. We tested 10 sea-state scenarios from Calm to Rough sea (wave height up to $4\,\mathrm{m}$) with 100 randomized trials per scenario per method, in summary over 1 000 runs.

B. FAA Effect

The FAA method is demonstrated in Fig. 3. Without FAA, the UAV's attitude diverges from the USV's at touchdown, creating overturn risk. With FAA, attitude deviation is driven to near zero before contact regardless of instantaneous deck tilt.

C. Comparison with State of the Art

The summarized performance against MPC-NE [5] at Moderate sea is captured in Table I. MPC-FAA achieves $5\times$ smaller mean touchdown error, $2\times$ faster landing, and caps impact velocity below $1\,\mathrm{m\,s^{-1}}$ in all trials. Both MPC-FAA and MPC-NE methods were tested for 10 sea-state scenarios. The results are shown in Table II, addressing the wave period

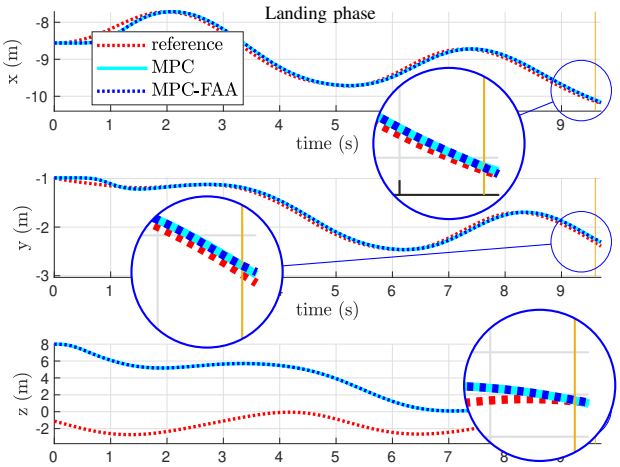

(a) Horizontal and vertical reference tracking.

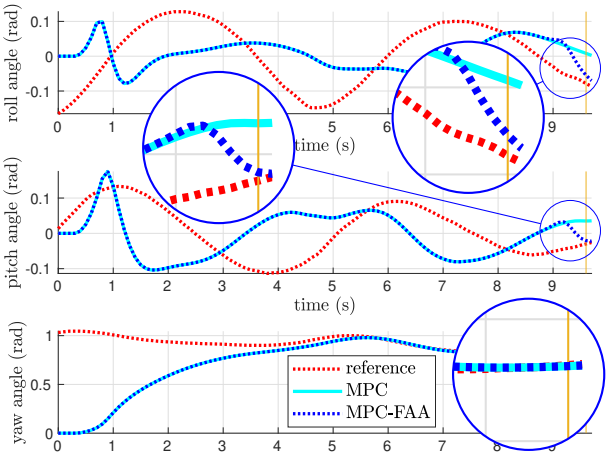

(b) UAV's attitude alignment upon the touchdown.

Fig. 3: Comparison of the MPC-based trajectory generator with FAA and without FAA in simulation at the LANDING phase. The vertical yellow line indicates a touchdown.

and amplitude used to simulate the sea. According to this table, MPC-FAA achieved a mean touchdown position closer to the center of the USV's deck across all tested scenarios when compared to MPC-NE. It needs to be noted that MPC-FAA recorded only 5 total failures versus 30 for MPC-NE.

TABLE I: Landing performance at Moderate sea (waves up to $2.5\,\mathrm{m}$), 100 trials per method. Position deviation is mean distance from deck center.

Metric	MPC-FAA (ours)	MPC-NE [5]
Success rate	**100 %**	95 %
Mean position deviation	$0.10\,\mathrm{m}$	$0.5\,\mathrm{m}$
Mean landing time	$17\,\mathrm{s}$	$34\,\mathrm{s}$
Pitch std. deviation	2.9°	3.4°
Roll std. deviation	2.3°	5.1°
Max impact velocity	$<1.0\,\mathrm{m\,s^{-1}}$	$2.0\,\mathrm{m\,s^{-1}}+$

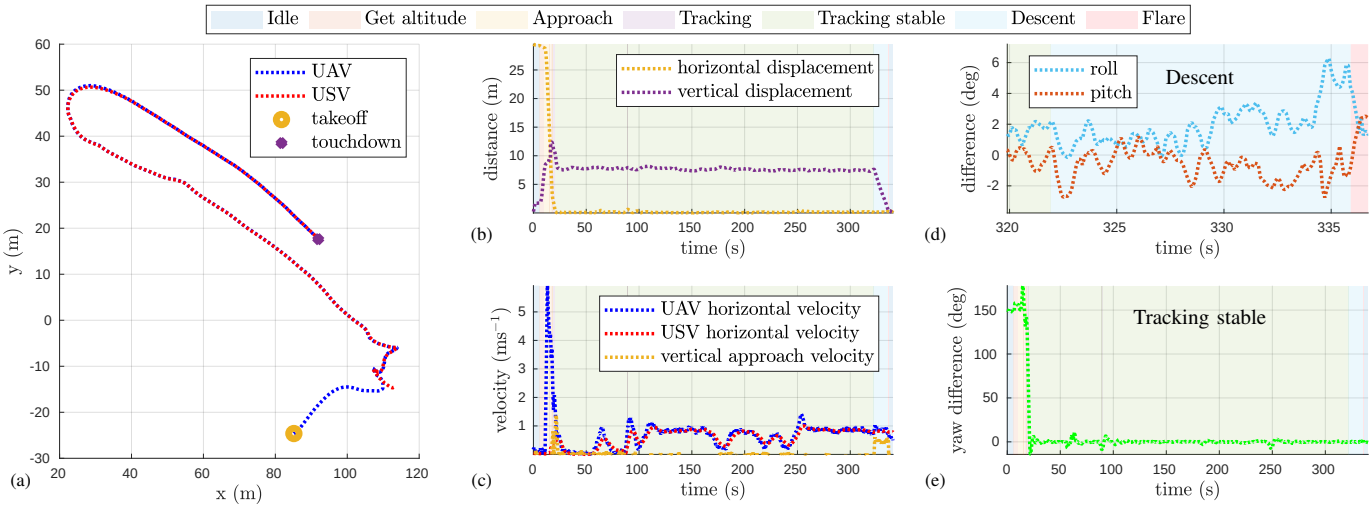

Fig. 4: Evaluation of the USV following and landing on its deck. Individual graphs depict (a) UAV's and USV's path with marked takeoff and touchdown positions, (b) position displacements between UAV and USV, (c) horizontal velocity together with vertical approach velocity, (d) the difference between the roll and pitch of the UAV and USV during `Descent` and `Flare` states, and (e) yaw difference between UAV and USV. Adopted from [10].

TABLE II: Landing performance across 10 sea-state scenarios.

Sea state	Amp.[1] (m)	Per.[2] (s)	Precision (m) FAA	Precision (m) NE	Duration[3](s) FAA	Duration[3](s) NE	Velocity[4](m/s) FAA	Velocity[4](m/s) NE
No waves	0.0	0.0	0.0	0.0	11.8	50.8	0.2	0.1
Slight	0.2	5.0	0.1	0.2	25.3	43.3	0.3	0.3
	0.3	5.0	0.1	0.3	18.7	43.9	0.3	0.4
Moderate	0.4	5.0	0.2	0.3	18.3	44.5	0.4	0.5
	0.4	4.0	0.3	0.4	24.6	43.1	0.5	0.4
	0.5	5.0	0.1	0.5	17.7	34.5	0.4	0.7
Rough	0.6	6.0	0.1	0.8	15.4	37.9	0.4	0.8
	0.7	7.0	0.2	0.3	15.4	33.2	0.5	0.5
	0.8	5.0	0.2	0.7	45.1	47.2	0.4	0.9
	0.8	8.0	0.4	0.5	18.2	41.9	0.6	0.4

[1] Amplitude
[2] Period
[3] Mean landing duration from descent initiation to touchdown.
[4] Mean touchdown velocity at the moment of deck contact.

D. REAL-WORLD Validation

Real-world experiments were conducted on freshwater reservoirs with an inflatable USV mockup subjected to artificially generated waves, ensuring repeatability independent of open-water weather conditions. The UAV platform uses a Tarot T650 frame with brushless Tarot 4114 320 KV motors, a Pixhawk 4 autopilot, and a LiPo 6S 8000 mAh battery. All autonomy software runs on an onboard Intel NUC i7 8559U (16 GB RAM). Localization fuses GNSS, Inertial Measurement Unit (IMU), AprilTag detection (RealSense D435 camera), and UVDAR relative localization (UV-LED markers and mvBlueFOX camera). The UAV legs are equipped with floats and all electronics protected with a water-resistant spray.

Figure 4 shows results from a representative experiment. The UAV navigates from over 90 m away, tracks the USV through a turning maneuver, and lands. With wind gusts up to 17 km h^{-1} and artificial waves inducing up to $\pm 8^\circ$ pitch and $\pm 6^\circ$ roll on the deck, the system lands with position deviation $\approx$ 15 cm and attitude deviation $< 2^\circ$ in all axes. Landing phases lasted 8–10 s. Results match the simulation closely, confirming that the method transfers to the real world without parameter retuning.

V. Conclusions

In this paper, we proposed a novel method for autonomous trajectory generation of UAV landing on top of a moving and rocking USV. The novel MPC-based trajectory generation relies on the accurate estimation and prediction of USV states, along with precise autonomous control of a UAV. Thanks to the dynamic modification of the penalization matrices, the vertical approach speed is reduced, and attitude angles are aligned with the USV to decrease the impact of the UAV's gear just before the touchdown. The UAV can successfully land in *Moderate sea* conditions or even on *Rough sea* conditions when using our approach. MPC-FAA achieved a reliability rate of 99.5 % in harsh conditions in simulated cases, whereas the state-of-the-art approach had 6 times more unsuccessful touchdowns. Moreover, the results of the proposed system indicate a substantial improvement in touchdown accuracy, achieving approximately twice better precision while also completing the landing maneuver 50 % faster than MPC-NE method. These outcomes highlight the efficiency of our approach in comparison to existing techniques. Moreover, the MPC-based trajectory generator for landing the UAV on the USV was verified by conducting numerous real-world experiments.

Acknowledgment

This work has been supported by the Technology Innovation Institute - Sole Proprietorship LLC, UAE, under the Research Project Contract No. TII/ARRC/2055/2021, CTU grant no SGS23/177/OHK3/3T/13 and the Czech Science Foundation (GAČR) under research project No. 23-06162M.

REFERENCES

[1] Z. Yang, X. Yu, S. Dedman, M. Rosso, J. Zhu, J. Yang, Y. Xia, Y. Tian, G. Zhang, and J. Wang, "Uav remote sensing applications in marine monitoring: Knowledge visualization and review," *Science of The Total Environment*, vol. 838, p. 155939, 2022.

[2] A. B. Junaid, A. Konoiko, Y. Zweiri, M. N. Sahinkaya, and L. Seneviratne, "Autonomous wireless self-charging for multi-rotor unmanned aerial vehicles," *Energies*, vol. 10, no. 6, 2017.

[3] DailyPicksandFlicks, "Drone crashes into boat and falls into waterdial," Aug. 2016, accesed in January 2024. [Online]. Available: https://www.youtube.com/watch?v=sQVoPzJOcZw&t=60s&ab_channel=DailyPicksandFlicks

[4] T. I. Fossen, *Handbook of marine craft hydrodynamics and motion control*. John Wiley & Sons, 2011.

[5] P. M. Gupta, E. Pairet, T. Nascimento, and M. Saska, "Landing a uav in harsh winds and turbulent open waters," *IEEE Robotics and Automation Letters*, vol. 8, no. 2, pp. 744–751, 2022.

[6] Z.-C. Xu, B.-B. Hu, B. Liu, X. Wang, and H.-T. Zhang, "Vision-based Autonomous Landing of Unmanned Aerial Vehicle on a Motional Unmanned Surface Vessel," in *2020 39th Chinese Control Conference (CCC)*, 2020, pp. 6845–6850.

[7] S. Abujoub, J. McPhee, and R. A. Irani, "Methodologies for landing autonomous aerial vehicles on maritime vessels," *Aerospace Science and Technology*, vol. 106, p. 106169, 2020.

[8] F. Novak, T. Baca, O. Prochazka, and M. Saska, "State estimation of marine vessels affected by waves by unmanned aerial vehicles," 2024, Accessed in June 2024. [Online]. Available: https://mrs.fel.cvut.cz/data/papers/2024_Novak.pdf

[9] T. I. Fossen, "Marine control systems–guidance. navigation, and control of ships, rigs and underwater vehicles," *Marine Cybernetics, Trondheim, Norway, Org. Number NO 985 195 005 MVA, www. marinecybernetics. com, ISBN: 82 92356 00 2*, 2002.

[10] O. Procházka, F. Novák, T. Báča, P. M. Gupta, R. Pěnička, and M. Saska, "Model predictive control-based trajectory generation for agile landing of unmanned aerial vehicle on a moving boat," *Ocean Engineering*, vol. 313, p. 119164, 2024.

[11] L. Yang, Z. Liu, X. Wang, G. Wang, X. Hu, and Y. Xi, "Autonomous Landing of a Rotor Unmanned Aerial Vehicle on a Boat Using Image-Based Visual Servoing," in *2021 IEEE International Conference on Robotics and Biomimetics (ROBIO)*, 2021, pp. 1848–1854.

[12] W. Ding and H. Huang, "Research on dynamic landing guidance algorithm for the maritime quadrotor," *Ocean Engineering*, vol. 271, p. 113775, 2023.

[13] E. Olson, "AprilTag: A robust and flexible visual fiducial system," in *Proceedings of the IEEE International Conference on Robotics and Automation (ICRA)*. IEEE, May 2011, pp. 3400–3407.

[14] Y. Zhang, Z. Wu, and T. Wei, "Precise landing on moving platform for quadrotor uav via extended disturbance observer," *IEEE Transactions on Intelligent Vehicles*, pp. 1–10, 2024.

[15] S. Abujoub, J. McPhee, C. Westin, and R. A. Irani, "Unmanned Aerial Vehicle Landing on Maritime Vessels using Signal Prediction of the Ship Motion," in *OCEANS 2018 MTS/IEEE Charleston*, 2018, pp. 1–9.

[16] T. K. Venugopalan, T. Taher, and G. Barbastathis, "Autonomous landing of an unmanned aerial vehicle on an autonomous marine vehicle," in *2012 Oceans*, 2012, pp. 1–9.

[17] J. Stephenson, N. T. Duncan, and M. Greeff, "Distributed model predictive control for cooperative multirotor landing on uncrewed surface vessel in waves," *arXiv preprint arXiv:2402.10399*, 2024.

[18] G. V. Raffo, M. G. Ortega, and F. R. Rubio, "An integral predictive/nonlinear H_∞ control structure for a quadrotor helicopter," *Automatica*, vol. 46, no. 1, pp. 29–39, 2010.

[19] J. Rawlings, "Tutorial overview of model predictive control," *IEEE Control Systems Magazine*, vol. 20, no. 3, pp. 38–52, 2000.

[20] V. Walter, M. Saska, and A. Franchi, "Fast mutual relative localization of uavs using ultraviolet led markers," in *2018 International Conference on Unmanned Aircraft Systems (ICUAS)*. IEEE, 2018, pp. 1217–1226.

[21] J. Tessendorf, "Simulating ocean water," *Simulating nature: realistic and interactive techniques. SIGGRAPH*, vol. 1, no. 2, p. 5, 2001.

[22] T. Baca, M. Petrlik, M. Vrba, V. Spurny, R. Penicka, D. Hert, and M. Saska, "The MRS UAV System: Pushing the Frontiers of Reproducible Research, Real-world Deployment, and Education with Autonomous Unmanned Aerial Vehicles," *Journal of Intelligent & Robotic Systems*, vol. 102, no. 26, pp. 1–28, 05 2021.